Colloids and Surfaces B: Biointerfaces 150 (2017) 1–7

Contents lists available at ScienceDirect

Colloids and Surfaces B: Biointerfaces

journal homepage: www.elsevier.com/locate/colsurfb

# Synergistic effect of polyaniline coverage and surface microstructure on the inhibition of *Pseudomonas aeruginosa* biofilm formation

L.A. Gallarato[a], L.E. Mulko[b], M.S. Dardanelli[a], C.A. Barbero[b], D.F. Acevedo[b,*], E.I. Yslas[a,*]

[a] Departamento de Biología Molecular, Universidad Nacional de Río Cuarto-CONICET, Agencia Postal No. 3, X580BYA Río Cuarto, Argentina
[b] Departamento de Química, Universidad Nacional de Río Cuarto-CONICET, Agencia Postal No. 3, X580BYA Río Cuarto, Argentina

ARTICLE INFO

*Article history:*
Received 19 May 2016
Received in revised form 5 November 2016
Accepted 7 November 2016
Available online 9 November 2016

*Keywords:*
*Pseudomonas aeruginosa*
Adhesion
Polyaniline
Microstructured surface
Antimicrobial

ABSTRACT

Biofilm Formation is a survival strategy for microorganisms to adapt to their environment. Microbial cells in biofilm become tolerant and resistant to antibiotics and immune responses, increasing the difficulties for the clinical treatment of microbial infections. The surface chemistry and the micro/nano-topography of solid interfaces play a major role in mediating microorganism activity and adhesion. The effect of the surface chemical composition and topography on the adhesion and viability of *Pseudomonas aeruginosa* was studied. Polymeric (polyethylene terephthalate) surfaces were covered with a conducting polymer (polyaniline, PANI) film by *in-situ* polymerization and microstructured by Direct Laser Interference Patterning (DLIP). The viability of *Pseudomonas aeruginosa* on the different surfaces was investigated. The physicochemical properties of the surfaces were characterized by water contact angle measurements, scanning electron microscopy and atomic force microscopy. Bacterial biofilms were imaged by atomic force and scanning electron microscopies. The bacterial viability decreased on PANI compared with the substrate (polyethylene terephthalate) and it decreased even more upon micro-structuring the PANI films. In addition, the biofilm reduction could be improved using polymers with different chemical composition and/or the same polymer with different topographies. Both methods presented diminish the bacterial attachment and biofilm formation. These findings present a high impact related to materials for biomedical engineer applications regarding medical devices, as prostheses or catheters.



## 1. Introduction

The colonization by *Pseudomonas aeruginosa* on medical foreign bodies or indwelling devices is one of the main hospital-acquired associated infections [1]. Moreover, this ubiquitous organism causes nosocomial infections in immunocompromised patients [2]. It is accepted that microbial populations use cell attachment to solid substrates to survive, forming structured communities called biofilms. Biofilms are defined as a coherent cluster of bacterial cells embedded in a biopolymer matrix [3]. Biofilms of *P. aeruginosa* are formed from individual planktonic cells in a complex and highly regulated developmental process. The process of infection caused by bacteria on the biomaterials includes several steps: bacteria adhesion, growth and multiplication, and then biofilm formation by a thick layer of exopolysaccharide matrix secreted by the bacterial cells. The bacteria living in biofilms persist and resist adverse environmental conditions developing antimicrobials resistance. For this reason, microbial biofilms on medical devices are extremely difficult to treat. Furthermore, bacterial infections are probably the most common and challenging post-surgical complications affecting biomedical implants [4]. In that sense, biofilm formation on implanted surfaces is one of the major causes of implant failure [5]. This microbe often causes persistent and chronic infections in human patients who have catheters, prostheses or other similar devices and those with compromised immune systems [6,7]. The prevention of bacterial adhesion and biofilm formation on the material surfaces is a major clinical importance topic. One crucial step in biofilm development is the initial bacteria interaction with the surfaces that can ultimately lead to colonization and infection by pathogenic bacteria [8]. The surfaces bacterial attachment prevention is critical for the reduction of infections associated with indwelling biomedical devices. Nowadays, it is extremely important to develop advanced multifunctional materials with improved biocompatibility. While antibiotics and local biocides (*e.g.* silver ions) can be used, those soluble agents could cause unwanted effects in other organs of the patient. Therefore, it is important to develop bioactive material surfaces, which inhibit not only bac-

* Corresponding authors.
*E-mail addresses:* dacevedo@ing.unrc.edu.ar, dacevedo@exa.unrc.edu.ar (D.F. Acevedo), eyslas@exa.unrc.edu.ar (E.I. Yslas).

http://dx.doi.org/10.1016/j.colsurfb.2016.11.014
0927-7765/

terial adhesion but also biofilm formation. PANI is a well-known inherently conducting polymer which is insoluble in water. Recent reports have been exploring the antimicrobial properties of PANI in solution [9–12]. However, to the best of our knowledge, there are not previous reports regarding the inhibitory capacity of PANI films. Another strategy to combat bacterial biofouling is to modify the surface topography limiting the ability of individual cells to attach, colonize, and form biofilms [13]. The microtopography and architecture surface are important factors that could control the bacterial attachment. It has been confirmed that the topography modulates cellular functions at the cell-substrate interface [14]. Multiple research groups have demonstrated that micro and nano-topographies significantly reduce bacterial biofilms [15,16]. This study proposes to evaluate the effect of the chemically different substrates (PANI and PET) and the influence of the topography modification on PANI surface related to the biofilms formation and cell adhesion of *P. aeruginosa*.

In order to modify the topography of PANI, a laser ablation technique known as Direct Laser Interference Patterning (DLIP) was employed [17]. DLIP is useful to fabricate surface periodic structures with the advantage that neither molds nor masks are necessary to obtain the final structure [18,19]. In DLIP, an interference pattern is created by overlaying two or more coherent laser beams, which can be transferred directly onto the material surface. Due to the laser intensity at the interference maxima positions, polymers, metals, ceramics, and coatings can be patterned [20]. The structuring procedure is made in air and is compatible with sterile conditions.

In summary, the purpose of the present study is to investigate the antimicrobial effects of polyethylene terephthalate films modified with polyaniline and micro-structured PANI by DLIP against *Pseudomonas aeruginosa.* Based on the results, it is possible to conclude that bacterial adhesion was reduced on PANI films and it was even more reduced on micro-structured PANI films compared with polyethylene terephthalate films. As a consequence, the new surface could be extremely useful to keep bacteria off medical devices.

## 2. Materials and methods

### 2.1. Synthesis of polyaniline films

Polyaniline (PANI) films were obtained by *in-situ* polymerization of aniline onto polyethylene terephthalate (PET) [21]. Commercial films of PET were submerged in an aqueous solution containing 50 mM aniline. To initiate the polymerization, ammonium persulfate (APS) as an oxidant (50 mM) was added. Film pieces were left to react 2 h at room temperature. The polymerized films were rinsed thoroughly with a solution 1 M of hydrochloric acid. Then, the films were washed with deionized water (DI), dried with air and stored at room temperature. Finally, these films were sterilized overnight under UV light and using laminar flow.

### 2.2. Direct laser interference patterning experiments (DLIP)

A high-power pulsed Nd:YAG (Brilliant B 10, Quantel) with a wavelength of 355 nm, frequency of 10 Hz, and pulse duration of 10 ns was used for all interference experiments. A scheme of the experimental set-up was described in a preceding study [22]. The laser beams are guided to overlap on the samples surface by using different optical elements including mirrors, beam splitters, and lenses. For all the experiments the sample was irradiated with only one laser pulse. Line-like patterns with c.a. 1 μm were fabricated on all samples.

### 2.3. Contact angle measurements

The sessile drop method was employed to measure the static contact angles with DI water on different films. The measurements were carried out at 25 °C, using 2 μl of DI water deposited onto the surface. A digital microscope (Intel Play QX3) with a 60 X objective was used for photographing the drop image from the side while illuminated by a white LED light [23]. The images were analyzed using Drop Analysis add-in from ImageJ® image processing software.

The snake based approach was used to determinate the contact angle value [24]. This method is suitable for a very wide range of applications (*e.g.* non-axisymmetric drops, tilted drops, projected drops). It is based on a cubic B-spline snake whose minimum-curvature property allows a good description of drop contours with a limited number of control points. At least five readings (n = 5) were made on random parts of the films and the results informed are the average of these measurements.

### 2.4. Bacterial culture

*P. aeruginosa* (strain ATCC 15692/PAO1) was used as strain models in this study. The bacterial strains were streaked and grown overnight under aerobic conditions (16 h) at 37 °C in Luria Broth (LB) agar plates from frozen stock. One colony of each strain was inoculated in 20 mL LB medium overnight at 37 °C with shaking. This culture was used as source for the experiments and it was statically incubated and reduced to a final density of $1 \times 10^6$ CFU/mL determined by comparing the OD600 of the sample with a standard curve relating OD600 to cell number.

### 2.5. Quantification of biofilm formation by crystal violet staining

Biofilms were assayed by crystal violet staining [25]. Samples were sterilized under UV light overnight. The control film (PET), the PET film functionalized with polyaniline (PET-PANI) and the micro-structured PET film functionalized with polyaniline (PET-PANI-M) were put into 96 well plates, and 100 μl of $1 \times 10^6$ CFU/mL floating bacterial suspension was added to each well as previous authors had employed [26–29]. The microtiter-plate tests were incubated aerobically for 24 h at 37 °C. After that, the bacterial biofilms were evaluated by crystal violet staining. For this purpose, the floating bacterial suspension in the wells was removed. Then, the suspension was rinsed gently several times with PBS (phosphate buffer solution) to remove the non-adherent bacteria. The samples were stained with crystal violet dye (0.1% w/v), incubated at room temperature for 10–15 min, and rinsed repeatedly again with water. The wells were air-dried and the crystal violet retained in each well was solubilized by adding 33% acetic acid. The solutions in acetic acid were transferred to new 96-well plates. The crystal violet absorption (optical density at 595 nm, OD 595) was monitored using a microtiter plate reader (Bio-Rad), These OD 595 values were considered as an index of bacteria adhering to the surface and forming biofilms. Five independent experiments were performed in triplicatesand the data was then averaged and the standard deviation was calculated.

### 2.6. Determination of the number of viable adhered cells

The three tested surfaces (PET, PET-PANI, and PET-PANI-M films) were gently rinsed with 1 mL of physiological saline solution (0.85 g of NaCl in 100 mL of DI water) to remove any non-adherent *P. aeruginosa* cells. The samples were vigorously rinsed with 1 mL of the same solution to remove all the adhered bacteria and were vortexed for 10 min. After preparation of serial dilutions, the bacterial counts were determined by plating on LB agar incubated at 37 °C for 24 h. Five independent experiments were carried out in tripli-

cate. A total viable count was performed for each surface and the total CFUs average determined using LB agar plates.

### 2.7. Determination of the dead and live cells

The live/dead bacteria was evaluated using a Live/Dead® Baclight™ bacterial viability kit (Life Technologies, Carlsbad, CA, USA). Bacteria viability tests for PET, PET-PANI, and PET-PANI-M films were performed. The films were incubated with *Pseudomonas aeruginosa* cells ($1 \times 10^6$) in physiological saline solution for 48 h at 37 °C to study the possible effect of the re-colonization. The incubation time employed was 48 h at the same mentioned temperature. Then, the samples were washed three times with 0.9% NaCl to remove any non-adherent *P. aeruginosa* cells, and staining according to the manufacturer specifications. Cells were finally examined under fluorescence microscopy (Nikon Eclipse 50i). The light microscopy system was additionally equipped with filters to acquire epifluorescence images of the live (green fluorescent) and dead (red fluorescent) cells. The viability of the bacteria was determined as the ratio between the viable and the total number of bacteria. The informed percentage of live and dead cells was calculated based on the average of three independent experiments using ImageJ® software, employing at least five microscope fields for every sample.

### 2.8. Bacterial observation by scanning electron microscopy (SEM) and atomic force microscopy (AFM)

The bacterial attachment to PET-PANI and PET-PANI-M was analyzed using different microscopic techniques including SEM and AFM. Bacteria were harvested and fixed in 2% glutaraldehyde and sputter-coated with gold according to standard procedures [30]. The SEM images were obtained with a Philips XL Feg 30 SEM operated at 2–5 kV accelerating tension.

The films with adherent bacterial cells were fixed with 2% glutaraldehyde for 1 h. Then the films were rinsed three times with water to remove the residual glutaraldehyde solution before were observed by AFM. The atomic force microscopy measurements were made with an Agilent 5420 AFM/STM microscope. A commercial Point Probe® Plus Contact/Tapping Mode with a force constant of 6 N $m^{-1}$, 156 Hz was used in non-contact mode.

### 2.9. Statistical analysis

All results were expressed as the mean values ± standard deviation (SD). The statistical analysis was carried out on different samples using one-way analysis of variance (ANOVA) followed by post hoc statistical tests, using the Tukey test for each pair of compared groups ($p < 0.05$ was considered significant).

## 3. Results and discussion

### 3.1. Contact angle measurements

Evaluation of surface hydrophobicity was performed by measuring the contact angle of water with the surfaces. The water drops contact angle values for the base material (PET), the material modified with PANI (PET-PANI) and the microstructured PANI on PET (PET-PANI-M) are shown in Table 1. The measured contact angle for commercial PET film was 72° ± 1.1° which was similar to that reported by Inagaki et al. (73°) [31]. The measured contact angle of PANI is 84° ± 3.0°. Stetjal et al. and Shishkanova et al. have reported a water contact angle for PANI of 82° [32,33]. The value indicates that PANI is more hydrophobic than PET. The contact angle of microstructured PANI is 101° ± 1.0°. The PET-PANI-M surface showed and increased apparent hydrophilicity.

**Table 1**
Water contact angle values (WCA) of PANI, PET-PANI and PET-PANI-M.

| Surface | WCA |
|---|---|
| PET | 72° ± 1.1 |
| PET-PANI | 84° ± 3.0 |
| PET-PANI-M | 101° ± 1.0 |

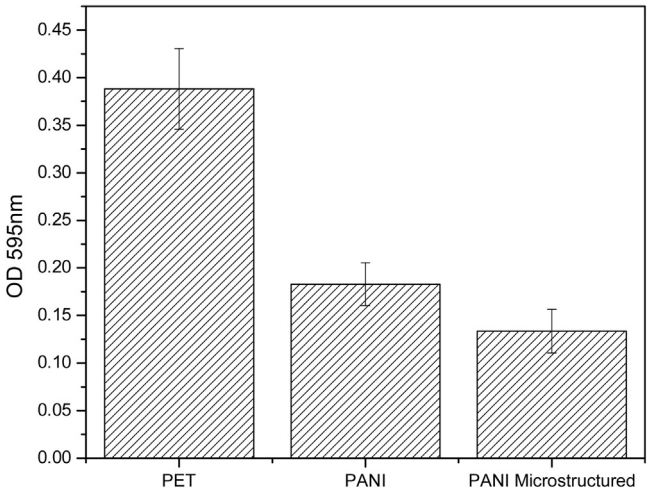


**Fig. 1.** Quantification of Biofilm formation on PET, PET-PANI and PET-PANI-M films after 24 h of growth by OD595. The data are the average of five independent experiments performed in triplicate, and the standard deviation is shown. Error bars represent mean ± SD,* $p < 0.05$ and ** $p < 0.01$.

Previous studies on the wettability of surfaces treated with laser show variations in the contact angle values [34,35]. Hans et al. have demonstrated changes in the wetting properties of surfaces induced by the microstructuring using DLIP [35]. These authors established that the microstructuring of a polyimide surface by DLIP could increase the contact angle from 68° up to 110° [35]. The PET-PANI-M surface follows the same behavior that polyimide and do not follow Wenzel model [36]. This law predicts a hydrophilicity rise (lower contact angle) when the surface roughness increase for an initially hydrophilic material. The increase of the contact angle with the rising surface roughness is contemplated by the Cassie and Baxter wetting model [37]. However, this theory is applied to surfaces with contact angle < 90°. In that sense, not only surface energy and average roughness seem to be the main parameters, other parameters should be taking into account such as pattern periodicity, geometrical form of the structures, etc. [35]. The results obtained for PET-PANI-M clearly demonstrate that the structure increases the contact angle regardless of its initial hydrophilic character, suggesting the presence of trapped air pockets according to Cassie and Baxter model.

Table 1 Water contact angle values (WCA) of PANI, PET-PANI and PET-PANI-M

### 3.2. Quantification of biofilm formation by crystal violet staining

The quantification of the biofilm formation by crystal violet staining is presented in Fig. 1. The *P. aeruginosa* on PET films show a strong biofilm formation with an optical density average measured at 595 nm (OD 595) of 0.380 ± 0.042. When the PET is modified by PANI the OD 595 value is 0.183 ± 0.022 and the same film topologically modified by DLIP shows fewer biofilms formation with an OD 595 value of 0.133 ± 0.022. The results show significant reductions in biofilm formation (c.a. 52%) when PET and PET-PANI films are compared. Besides, by comparison of biofilms formation of PET and PET-PANI-M films, it is possible to conclude that the reduction

**Table 2**
Bacteria viable cells quantity grown for 24 h (CFU/mL), bacterial adhesion reduction ratio (LAR), adhesion reduction percentage (% $R_{ad}$), and adhesion percentage (% Ad) on different films.

| Surface | CFU/mL | Log CFU/mL | LAR | % $R_{ad}$ | % Ad |
|---|---|---|---|---|---|
| PET | $1.78 \times 10^8$ | 8.24 | 0 | 0 | 100 |
| PET-PANI | $4.54 \times 10^7$ | 7.65 | 0.59 | 74.30 | 25.70 |
| PET-PANI-M | $4.45 \times 10^6$ | 6.65 | 1.59 | 97.43 | 2.52 |

in biofilm formation due to PANI coverage and microstructuring reaches 64%. This evidence suggests that PANI is the major biofilm inhibition agent and a synergistic effect is generated by the microstructuration of PANI surface.

### 3.3. Bacterial adhesion and growth

In order to determinate the viable cells quantity; bacteria were counted after different dilutions and incubated on LB Agar at 37 °C for 24 h. The developed colonies were counted and converted to colony forming unit per milliliter (CFU/mL). The informed CFU/mL values are the average of five measurements of three independent experiments.

In this work, the adhesion reduction between two different films (PET and PET-PANI or PET-PANI-M) is quantified using the bacterial adhesion reduction ratio (LAR) following Eq. (1) [38].

$$LAR = \log\left[\frac{\left(\frac{CFU}{mL}\right)_{PET}}{\left(\frac{CFU}{mL}\right)_{OF}}\right] \quad (1)$$

Where $(CFU/mL)_{PET}$ is the bacteria colony forming unit value per milliliter on PET, $(CFU/mL)_{OF}$ is the bacteria colony forming unit value per milliliter on the modified polymers (PET-PANI or PET-PANI-M). Also, the adhesion reduction percentage ($\%R_{ad}$) between the control film (PET) and the modified films (PET-PANI or PET-PANI-M) are expressed in percentage logarithm and it was calculated using Eq. (2).

$$\%R_{ad} = \left(1 - 10^{-LAR}\right) x100 \quad (2)$$

As it can be seen, after 24 h incubation, *P. aeruginosa* cells are able to colonize all the surfaces exposed, PET, PET-PANI and PET-PANI-M films. However, the results show that gram-negative *P. aeruginosa* growth is reduced in a 74.3%; from 8.24 Log CFU/mL on PET to 7.65 Log CFU/mL on PET-PANI suggesting a chemical-induced effect. While a decreases of 23.13%, from 7.65 Log CFU/mL to 6.65 Log CFU/mL, is observed when PET-PANI are compared with PET-PANI-M films suggesting, in this case, a topographical-induced effect (see Table 2). A synergistic effect can be observed when the Log CFU/mL PET value (8.24) is compared with Log CFU/mL PET-PANI-M value (6.65). The results demonstrate that the PET surface modified by covering with a PANI film which is microstructured by DLIP show a reduction of adhesion of 97.43% due to chemical and topographic effects. The percentage of adhesion (% Ad) can be defined as the percentage of the adhering cells on PET-PANI or PET-PANI-M related to those adhering on PET control film. It was estimated using Eq. (3).

$$\%Ad = 100 - \%R_{ad} \quad (3)$$

The results show a% Ad is of 25.70% for PET-PANI and only 2.52% on PET-PANI-M. A clear inhibition of surface bacterial growth is observed as can be seen in Table 2. In that sense, on PET-PANI surface, the adhesion of the living bacteria is diminished by one order of magnitude (in CFU/mL). On PET-PANI-M this reduction value reaches 1.59 order of magnitude (in CFU/mL). PET-PANI surface significantly decreases the attachment and growth of the gram-negative species *P. aeruginosa* after 1 day of culture compared with PET surfaces.

Table 2 Bacteria viable cells quantity grown for 24 hs (CFU/mL), bacterial adhesion reduction ratio (LAR), adhesion reduction percentage (% $R_{ad}$) and adhesion percentage (% Ad), on different films.

The quantification of the live and dead cells in the samples was also studied by fluorescent-based cell live/dead test. The live and dead bacterial cells were subsequently conducted to visually demonstrate cell integrity disruption on the different surfaces cultivated with *P. aeruginosa* as model bacteria for 48 h at 37 °C, see Fig. 2.

The number of live cells on PET films, 80 ± 1.5%, is higher than the dead cells (Fig. 2a–c). The test results for the surface modified with PANI show that the percentage of the live cells decreases 44 ± 1% compared with PET film. Moreover, the live cells percentage (45 ± 2%) is lower that the dead ones (54 ± 2%) in the same film. The analysis of the PANI-PET-M images, Fig. 2d–f, show that the live cells adhered percentage is lower than the other surfaces (35 ± 1%); and the dead cell percentage (63 ± 2%) is higer that on PET and PET-PANI. The experiments carried out during 48 h present the same tendency that the adhesion results obtained using violet crystal and allow to conclude that the bacateria can not re-cololize the surface. The results of this study are in agreement with the percentage of the adhered cells, the quantication of the cell in the images shows an adhesion reduction of 50% and 60% for PET-PANI and PET-PANI-M. Therefore, it is possible to conclude that bacterial viability and adhesion are reduced on the PET-PANI and strongly reduced on PET-PANI-M compared to PET surface.

### 3.4. Bacterial observation by SEM and AFM

In Fig. 3a is shown the SEM micrograph of a microstructured PANI film on PET. As it can be seen in the image, the topography generated using DLIP on PANI is highly uniform. The technique produces regular patterning lines on the surface with a period of c.a. 1 μm and a height of c.a. 220 nm (Fig. 3b). Lines area easy to patterning using DLIP with only two beams. Additionally, the presence of trenches between lines allows to see if 2D anisotropy of the surface affects the shape of the bacteria and/or bacterial clusters.

The analysis of SEM (Fig. 4a–c) and AFM (Fig. 4d–f) images reveal different attachment responses of *P. aeruginosa* grown (for 24 h) on the tested substrates. *P. aeruginosa* on a PET (Fig. 4a and d) and PET-PANI (Fig. 4b and e) surface are random and isotropically distributed. The images shown in Fig. 4c and f reveal that the majority of the attached cells to PET-PANI-M are oriented parallel to the direction of channels. Moreover, it can be seen that the bacteria are preferably attached inside the channels between the DLIP generated ridges (Fig. 4c and f). The results presented in this study suggest that bacterial cells, grown for 24 h, are able to differentiate upper and lower areas in spatially organized microtopographic surface structures. It is proposed that such preferred cell orientation reflects the influence of the microscale structure. It is known that, abundant production of extracellular polymeric substances (EPS) is generated by bacteria in order to form the biofilm [39]. This behavior is an overall phenomenon that can control natural biofilm organization at the cellular level. When the bacteria grow in the topographically modified films there are mostly separated and it can not generate compact biofilms in the first stage of growth. It is likely that different cells cannot build an extracellular film trough the PANI ridges and remain isolated inside the channels. Further, it is clear that surface topography enhance the effect produced by the chemical modification on bacterial biofilm inhibition. The results showed that bacteria attachment on the two kinds of PANI surfaces is quite different. In summary, taking into account the results obtained at 24 h (Fig. 4c and f) it is possible to conclude that the cells in the first stage of growth are aligned with the patterns but at longer time of incubation (48 h, Fig. 2g–i), the bacteria do not present a preferencial orientation on the microstructured surface.

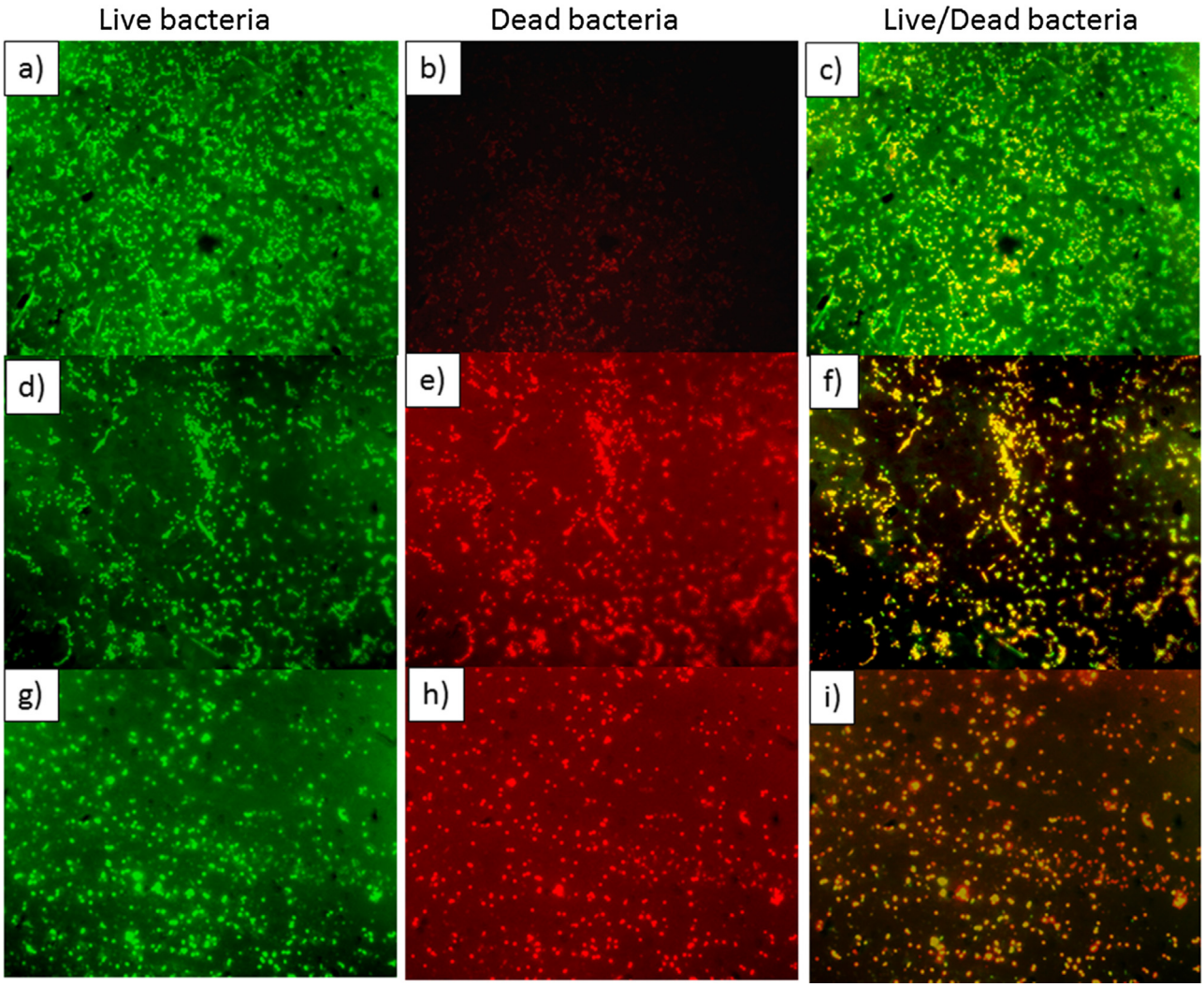


**Fig. 2.** Epifluorescence digital images of the live (green fluorescent) and dead (red fluorescent) cells grown for 48 h on a–c) PET, d–f) PET-PANI and g–i) PET-PANI-M. (For interpretation of the references to colour in this figure legend, the reader is referred to the web version of this article.)

This behavior could explain the adhesion and biofilm formation disminusion related to unmodified PANI film.

It has been shown that mouse mammary adenocarcinoma cells grow aligned to the direction of the patterns [40]. Here, the size of the bacterial cells allows for the formation of aligned rows of cells inside the trenches made by DLIP in the PANI film in the first stage of growth. In that sense, the findings regarding the surface architecture impact on the bacteria attachment are noteworthy. The present results confirm that it is possible to control the cell attachment not only for eukaryotic but also prokaryotic cells by tuning the surface topography and morphology through microstructure.

It has been found that PANI shows antibacterial properties [41,42]. The inhibition of bacterial growth obtained in the presen study also suggests that PANI has antibacterial properties through the inhibition on *P. aeruginosa* attachment and growth. Many strategies have been proposed to develop antibacterial surfaces

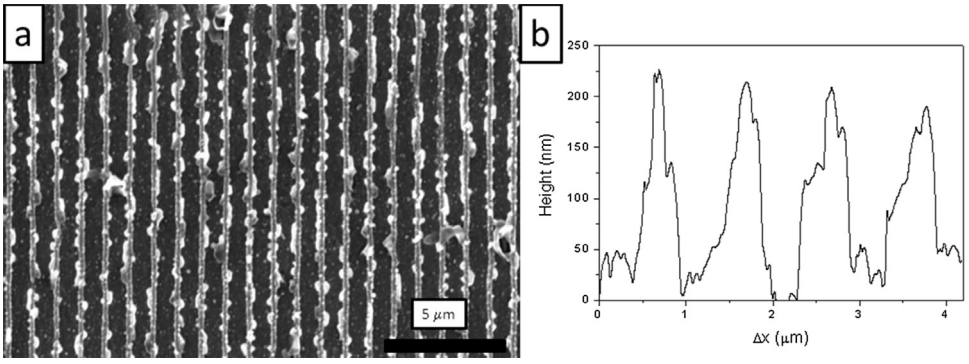


**Fig. 3.** a) Scanning electron microscopy micrographs of the PET-PANI-M film; b) Profile of the PET-PANI-M surface extracted by AFM image.

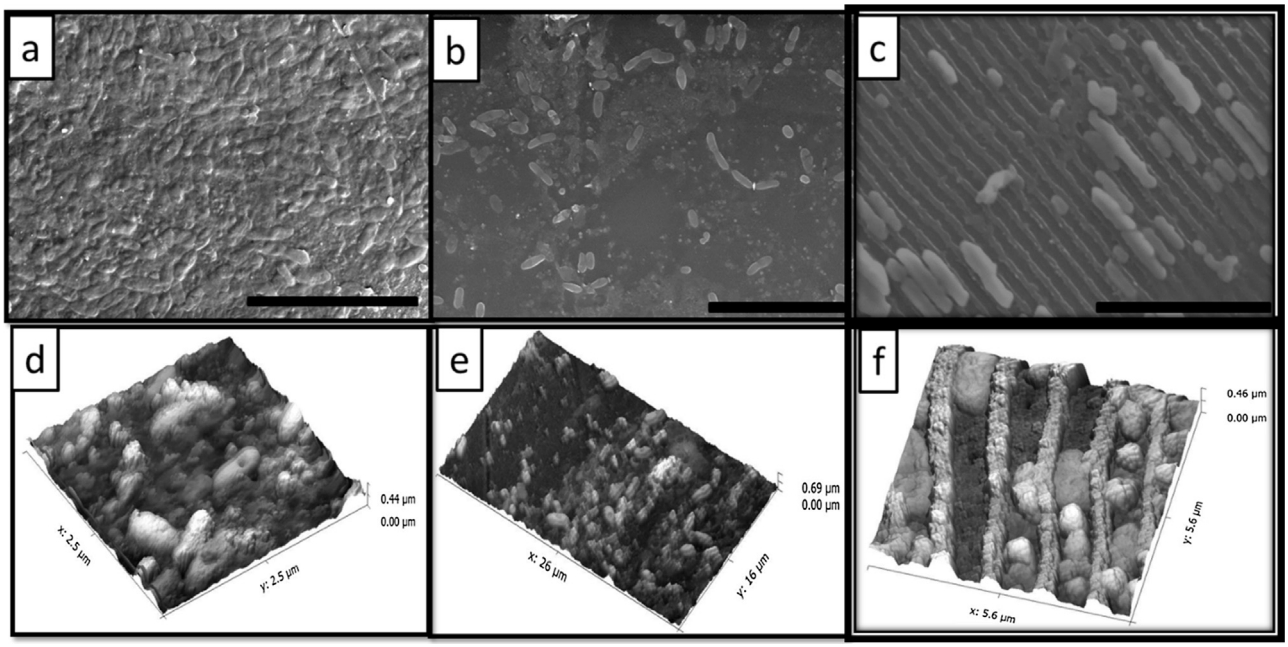


**Fig. 4.** a) Scanning electron microscopy (SEM) micrographs of the biofilm formed (grown for 24 h) on a) PET, b) PET-PANI film; c) PET-PANI-M scale bar 10 µm; and Atomic Force Microscopy (AFM) micrograph of the bacteria grown for 24 h on d) PET, e) PET-PANI and f) PET-PANI-M.

based on the physicochemical parameters of the surface, modifying the bacterial adhesion such as topography, charge, hydrophilic or hydrophobic [3,43–45]. Some of them are based on physical proprieties surface topography modification, generating micro or nano-structured surfaces [46–48]. The outcomes of this study are in agreement with these reports, thus confirming the hypothesis that surface morphology and topography strongly influence the bacterial attachment degree to surfaces. As it can be seen in Fig. 4 c and f, the appearance of the *P. aeruginosa* bacteria grown on PET-PANI-M shows a spherical shape. This behavior has been observed in other studies [49–51]. The authors showed that the change in *P. fluorescens* morphology was expressed when the microorganism are cultivated on structured surface [49]. The researchers demonstrate that the bacteria acts in response to the topography since they chose a preferential direction, changed their morphology and modified the production of exopolysaccharide under these conditions [50]. Moreover, Monahan et al. attributed the behavior to a strategy of the cell to survive when the microorganism is exposed to stress conditions [51].

In conclusion, the described results suggest that PANI inhibits the adhesion and growth of *P. aeruginosa* on surfaces, diminishing the biofilm formation. It was also shown that topographic changes synergically increase the inhibition of bacterial adhesion producing an overall antibacterial effect.

## 4. Conclusions

Bacterial adhesion and biofilm formation are remarkable concepts in medicine. It has been established that the main problem with infections caused by biofilms is the increased antibiotic resistance. In this work, it is demonstrated a simple method to change the chemical composition of PET surfaces (or other polymers) using *in-situ* polymerization of aniline. In that sense, the surfaces chemical modification with PANI produces strongly inhibition of the bacterial adhesion (more than 70%) and biofilms formation (more than 50%). Moreover, it is shown that microstructuring PANI by an easy to use technique (DLIP) synergically increases the PANI surface antimicrobial ability, decreasing the bacterial adhesion by c.a. 97.5% and the biofilm formation by c.a. 65%. A synergistic effect it is certainly demonstrated due to chemical and topological effects made onto PET control film; confirming that cellular interactions with surfaces are governed by multiple factors (chemistry, charge, mechanical properties, and topography). Also, it is shown that prokaryotic cells selectively grow inside PANI surface channels made by DLIP of PANI films in the first stage of growth. Finally, it is possible to conclude that the reduction biofilm-forming bacteria could be improved using polymers with different chemical composition and/or the same polymer with different topographies. These findings could be applied in biomedical engineering for the inhibition of bacterial infection due to medical devices, like prostheses or catheters.

## Acknowledgements

D.F. Acevedo E.I. Yslas, M. Dardanelli and C.A. Barbero, are permanent research fellows of CONICET. L. Mulko thanks CONICET for a graduate fellowships. The funding of FONCYT (PICT 2013-2716), CONICET (PIP 2014-2016, No. 11220130100663CO), SECYT-UNRC and EU (IRSES project “SUMA2-Network”, Pr. No: 318903) is gratefully acknowledged.

## References

[1] P.D. Lister, D.J. Wolter, N.D. Hanson, Antibacterial-resistant Pseudomonas aeruginosa: clinical impact and complex regulation of chromosomally encoded resistance mechanisms, Clin. Microbiol. Rev. 22 (2009) 582–610, http://dx.doi.org/10.1128/CMR.00040-09.
[2] R. Bou, A. Aguilar, J. Perpiñán, P. Ramos, M. Peris, L. Lorente, A. Zúñiga, Nosocomial outbreak of Pseudomonas aeruginosa infections related to a flexible bronchoscope, J. Hosp. Infect. 64 (2006) 129–135, http://dx.doi.org/10.1016/j.jhin.2006.06.014.
[3] K. Glinel, P. Thebault, V. Humblot, C.M. Pradier, T. Jouenne, Antibacterial surfaces developed from bio-inspired approaches, Acta Biomater. 8 (2012) 1670–1684, http://dx.doi.org/10.1016/j.actbio.2012.01.011.
[4] S.J. McConoughey, R. Howlin, J.F. Granger, M.M. Manring, J.H. Calhoun, M. Shirtliff, S. Kathju, P. Stoodley, Biofilms in periprosthetic orthopedic infections, Future Microbiol. 9 (2014) 987–1007, http://dx.doi.org/10.2217/fmb.14.64.
[5] L.J. Douglas, Candida biofilms and their role in infection, Trends Microbiol. 11 (2003) 30–36, http://dx.doi.org/10.1016/S0966-842X(02)00002-1.

[6] B. Foxman, Epidemiology of urinary tract infections: incidence, morbidity, and economic costs, Dis. Mon. 49 (2003) 53–70, http://dx.doi.org/10.1016/S0011-5029(03)90000-9.

[7] J.A. Ryan, R.M. Abel, W.M. Abbott, C.C. Hopkins, T.M. Chesney, R. Colley, K. Phillips, J.E. Fischer, Catheter complications in total parenteral nutrition, N. Engl. J. Med. 290 (1974) 757–761, http://dx.doi.org/10.1056/NEJM197404042901401.

[8] L. Hall-Stoodley, J.W. Costerton, P. Stoodley, Bacterial biofilms: from the natural environment to infectious diseases, Nat. Rev. Microbiol. 2 (2004) 95–108, http://dx.doi.org/10.1038/nrmicro821.

[9] M.R. Gizdavic-Nikolaidis, J.R. Bennett, S. Swift, A.J. Easteal, M. Ambrose, Broad spectrum antimicrobial activity of functionalized polyanilines, Acta Biomater. 7 (2011) 4204–4209, http://dx.doi.org/10.1016/j.actbio.2011.07.018.

[10] N. Shi, X. Guo, H. Jing, J. Gong, C. Sun, K. Yang, Antibacterial effect of the conducting polyaniline, J. Mater. Sci. Technol. 22 (2006) 289–290.

[11] M.R. Gizdavic-Nikolaidis, J.C. Pagnon, N. Ali, R. Sum, N. Davies, L.F. Roddam, M. Ambrose, Functionalized polyanilines disrupt Pseudomonas aeruginosa and Staphylococcus aureus biofilms, Coll. Surf. B Biointerfaces 136 (2015) 666–673, http://dx.doi.org/10.1016/j.colsurfb.2015.10.015.

[12] K. Pandiselvi, S. Thambidurai, Synthesis, characterization, and antimicrobial activity of chitosan–zinc oxide/polyaniline composites, Mater. Sci. Semicond. Process. 31 (2015) 573–581, http://dx.doi.org/10.1016/j.mssp.2014.12.044.

[13] J. Hasan, R.J. Crawford, E.P. Ivanova, Antibacterial surfaces: the quest for a new generation of biomaterials, Trends Biotechnol. 31 (2013) 295–304, http://dx.doi.org/10.1016/j.tibtech.2013.01.017.

[14] M. Nikkhah, F. Edalat, S. Manoucheri, A. Khademhosseini, Engineering microscale topographies to control the cell-substrate interface, Biomaterials 33 (2012) 5230–5246, http://dx.doi.org/10.1016/j.biomaterials.2012.03.079.

[15] M. Hoffman, R.M. May, S.T. Reddy, Micro-Patterned surfaces for reducing biofilm formation in an endotracheal-Tube-Like environment, Am. J. Infect. Control 40 (2012) e59–e60, http://dx.doi.org/10.1016/j.ajic.2012.04.103.

[16] J.F. Ling, M.V. Graham, N.C. Cady, Effect of topographically patterned poly(dimethylsiloxane) surfaces on Pseudomonas Adhesion and biofilm formation, Nano Life 02 (2012) 1242004, http://dx.doi.org/10.1142/S1793984412420044.

[17] D.A. Acevedo, A.F. Lasagni, C.A. Barbero, F. Mücklich, Simple fabrication method of conductive polymeric arrays by using direct laser interference micro-/nanopatterning, Adv. Mater. 19 (2007) 1272–1275, http://dx.doi.org/10.1002/adma.200601693.

[18] M.F. Broglia, D.F. Acevedo, D. Langheinrich, H.R. Perez-hernandez, C.A. Barbero, A.F. Lasagni, Rapid fabrication of periodic patterns on poly (styrene-co-acrylonitrile) surfaces using direct laser interference patterning, Int. J. Polym. Sci. 2015 (2015).

[19] D.F. Acevedo, E. Frontera, M.F. Broglia, F. Mücklich, M.C. Miras, C.a. Barbero, One step lithography of polypyrrole, Adv. Eng. Mater. 13 (2011) 405–410, http://dx.doi.org/10.1002/adem.201000295.

[20] A.F. Lasagni, D.F. Acevedo, C.A. Barbero, One-Step production of organized surface architectures on polymeric materials by direct laser interference patterning**, Adv. Eng. Mater. (2007) 99–103, http://dx.doi.org/10.1002/adem.200600171.

[21] P. Cavallo, D.F. Acevedo, M.C. Fuertes, G.J.a.a. Soler-Illia, C.a. Barbero, Understanding the sensing mechanism of polyaniline resistive sensors. Effect of humidity on sensing of organic volatiles, Sens. Actuators B Chem. 210 (2015) 574–580, http://dx.doi.org/10.1016/j.snb.2015.01.029.

[22] M. a. Molina, C.R. Rivarola, M.F. Broglia, D.F. Acevedo, C. a. Barbero, Smart surfaces: reversible switching of a polymeric hydrogel topography, Soft Matter. 8 (2012) 307, http://dx.doi.org/10.1039/c1sm06191g.

[23] E.I. Yslas, P. Cavallo, D.F. Acevedo, C.A. Barbero, V.A. Rivarola, Cysteine modified polyaniline films improve biocompatibility for two cell lines, Mater. Sci. Eng. C 51 (2015) 51–56, http://dx.doi.org/10.1016/j.msec.2015.02.049.

[24] A.F. Stalder, G. Kulik, D. Sage, L. Barbieri, P. Hoffmann, A snake-based approach to accurate determination of both contact points and contact angles, Coll. Surf. A Physicochem. Eng. Asp 286 (2006) 92–103, http://dx.doi.org/10.1016/j.colsurfa.2006.03.008.

[25] E. Burton, N. Yakandawala, K. LoVetri, M.S. Madhyastha, A microplate spectrofluorometric assay for bacterial biofilms, J. Ind. Microbiol. Biotechnol. 34 (2007) 1–4, http://dx.doi.org/10.1007/s10295-006-0086-3.

[26] H.P. Steinmetz, S. Rudnick-Glick, M. Natan, E. Banin, S. Margel, Graft polymerization of styryl bisphosphonate monomer onto polypropylene films for inhibition of biofilm formation, Coll. Surf. B Biointerfaces 147 (2016) 300–306, http://dx.doi.org/10.1016/j.colsurfb.2016.08.007.

[27] I. d'Angelo, B. Casciaro, A. Miro, F. Quaglia, M.L. Mangoni, F. Ungaro, Overcoming barriers in Pseudomonas aeruginosa lung infections: engineered nanoparticles for local delivery of a cationic antimicrobial peptide, Coll. Surf. B Biointerfaces 135 (2015) 717–725, http://dx.doi.org/10.1016/j.colsurfb.2015.08.027.

[28] J. Hernández-Montelongo, V.F. Nascimento, D. Murillo, T.B. Taketa, P. Sahoo, A.A. De Souza, M.M. Beppu, M.A. Cotta, Nanofilms of hyaluronan/chitosan assembled layer-by-layer: an antibacterial surface for Xylella fastidiosa, Carbohydr. Polym. 136 (2016) 1–11, http://dx.doi.org/10.1016/j.carbpol.2015.08.076.

[29] P. Bharali, J.P. Saikia, A. Ray, B.K. Konwar, Rhamnolipid (RL) from Pseudomonas aeruginosa OBP1: A novel chemotaxis and antibacterial agent, Coll. Surf. B Biointerfaces 103 (2013) 502–509, http://dx.doi.org/10.1016/j.colsurfb.2012.10.064.

[30] A.P. Ricomini Filho, F. Silva de Freitas Fernandes, F. Gouveia Straioto, W.J. da Silva, A.A. del Bel Cury, Preload loss and bacterial penetration on different implant-abutment connection systems, Braz. Dent. J. 21 (2010) 123–129, http://dx.doi.org/10.1590/S0103-64402010000200006.

[31] N. Inagaki, K. Narushima, A. Yokoi, Surface modification of PET films by a combination of vinylphthalimide deposition and Ar plasma irradiation, J. Adhes. Sci. Technol. 18 (2004) 1517–1528, http://dx.doi.org/10.1163/1568561042411213.

[32] T.V. Shishkanova, I. Sapurina, J. Stejskal, V. Král, R. Volf, Ion-selective electrodes: polyaniline modification and anion recognition, Anal. Chim. Acta 553 (2005) 160–168, http://dx.doi.org/10.1016/j.aca.2005.08.018.

[33] J. Stejskal, J. Prokes, M. Trchova, Reprotonation of polyaniline: a route to various conducting polymer materials, React. Funct. Polym. 68 (2008) 1355–1361, http://dx.doi.org/10.1016/j.reactfunctpolym.2008.06.012.

[34] B.T. Least, D.A. Willis, Modification of polyimide wetting properties by laser ablated conical microstructures, Appl. Surf. Sci. 273 (2013) 1–11, http://dx.doi.org/10.1016/j.apsusc.2012.12.141.

[35] M. Hans, C. Gachot, F. Müller, F. Mücklich, Direct laser interference structuring as a tool to gradually tune the wetting response of titanium and polyimide surfaces, Adv. Eng. Mater. 11 (2009) 795–800, http://dx.doi.org/10.1002/adem.200900115.

[36] R.N. Wenzel, Resistance of solid surfaces to wetting by water, J. Ind. Eng. Chem. (Washington, D. C.) 28 (1936) 988–994, http://dx.doi.org/10.1021/ie50320a024.

[37] A.B.D. Cassie, S. Baxter, Wettability of porous surfaces, Trans. Faraday Soc. 40 (1944) 546, http://dx.doi.org/10.1039/tf9444000546.

[38] A. Muazu, N.I.A. Rahman, U.F. Abdullahi, S. Aliyu, J.A. Ogidi, A.F. Umar, Assessment of chemical disinfectants efficacy against escherichia coli biofilm developed on glass and wood at refrigeration and room temperatures, J. Appl. Pharm. Sci. 5 (2015) 074–079, http://dx.doi.org/10.7324/JAPS.2015.501212.

[39] R.M. Donlan, Biofilms: microbial life on surfaces, Emerg. Infect. Dis. 8 (2002) 881–890, http://dx.doi.org/10.3201/eid0809.020063.

[40] D. Langheinrich, E. Yslas, M. Broglia, V. Rivarola, D. Acevedo, A. Lasagni, Control of cell growth direction by direct fabrication of periodic micro- and submicrometer arrays on polymers, J. Polym. Sci. Part B Polym. Phys. 50 (2012) 415–422, http://dx.doi.org/10.1002/polb.23017.

[41] P. Karunanithy, R.G.S.V. Prasad, V.S. Jakka, R.S.L. Aparna, A.R. Phani, G.S. Prabhakara, S.A. Ahmed, Enhanced antimicrobial activity of polyaniline grafted chitosan, Adv. Sci. Eng. Med. 5 (2013) 420–426, http://dx.doi.org/10.1166/asem.2013.1283.

[42] D.T. Seshadri, N.V. Bhat, Use of polyaniline as antimicrobial agent in textiles, Indian J. Fibre Text. Res. 30 (2005) 204–206.

[43] N. Mitik-Dineva, J. Wang, V.K. Truong, P. Stoddart, F. Malherbe, R.J. Crawford, E.P. Ivanova, Escherichia coli, pseudomonas aeruginosa, and staphylococcus aureus attachment patterns on glass surfaces with nanoscale roughness, Curr. Microbiol. 58 (2009) 268–273, http://dx.doi.org/10.1007/s00284-008-9320-8.

[44] X. Dai, J. Boll, M.E. Hayes, D.E. Aston, Adhesion of Cryptosporidium parvum and Giardia lamblia to solid surfaces: the role of surface charge and hydrophobicity, Colloids Surf. B Biointerfaces 34 (2004) 259–263, http://dx.doi.org/10.1016/j.colsurfb.2003.12.016.

[45] D. Davies, Understanding biofilm resistance to antibacterial agents, Nat. Rev. Drug Discov. 2 (2003) 114–122, http://dx.doi.org/10.1038/nrd1008.

[46] V.K. Truong, R. Lapovok, Y.S. Estrin, S. Rundell, J.Y. Wang, C.J. Fluke, R.J. Crawford, E.P. Ivanova, The influence of nano-scale surface roughness on bacterial adhesion to ultrafine-grained titanium, Biomaterials 31 (2010) 3674–3683, http://dx.doi.org/10.1016/j.biomaterials.2010.01.071.

[47] M. Graham, N. Cady, Nano and microscale topographies for the prevention of bacterial surface foulingg, Coatings 4 (2014) 37–59, http://dx.doi.org/10.3390/coatings4010037.

[48] A.V. Singh, V. Vyas, R. Patil, V. Sharma, P.E. Scopelliti, G. Bongiorno, A. Podestà, C. Lenardi, W.N. Gade, P. Milani, Quantitative characterization of the influence of the nanoscale morphology of nanostructured surfaces on bacterial adhesion and biofilm formtion, PLoS One 6 (2011) e25029, http://dx.doi.org/10.1371/journal.pone.0025029.

[49] C. Díaz, M.C. Cortizo, P.L. Schilardi, S.G.G. De Saravia, M.A.F.L. De Mele, Influence of the nano-micro structure of the surface on bacterial adhesion, Mater. Res. 10 (2007) 11–14, http://dx.doi.org/10.1590/S1516-14392007000100004.

[50] C. Díaz, P. Schilardi, M.F.L. De Mele, Influence of surface sub-micropattern on the adhesion of pioneer bacteria on metals, Artif. Organs 32 (2008) 292–298, http://dx.doi.org/10.1111/j.1525-1594.2008.00545.x.

[51] L.G. Monahan, L. Turnbull, S.R. Osvath, D. Birch, I.G. Charles, C.B. Whitchurch, Rapid conversion of Pseudomonas aeruginosa to a spherical cell morphotype facilitates tolerance to carbapenems and penicillins but increases susceptibility to antimicrobial peptides, Antimicrob. Agents Chemother. 58 (2014) 1956–1962, http://dx.doi.org/10.1128/AAC.01901-13.